Reaction Mechanism of the Acidic Hydrolysis of Highly Twisted Amides: Rate Acceleration Caused by the Twist of the Amide Bond

Jon I. Mujika, Elena Formoso, Jose M. Mercero, and Xabier Lopez*

Kimika Fakultatea and Donostia International Physics Center (DIPC), Euskal Herriko Unibertsitatea, 20080 Donostia, Euskadi, Spain

Received: January 19, 2006; In Final Form: April 26, 2006

We present an ab initio study of the acid hydrolysis of a highly twisted amide and a planar amide analogue. The aim of these studies is to investigate the effect that the twist of the amide bond has on the reaction barriers and mechanism of acid hydrolysis. Concerted and stepwise mechanisms were investigated using density functional theory and polarizable continuum model calculations. Remarkable differences were observed between the mechanism of twisted and planar amide, due mainly to the preference for N-protonation of the former and O-protonation of the latter. In addition, we were also able to determine that the hydrolytic mechanism of the twisted amide will be pH dependent. Thus, there is a preference for a stepwise mechanism with formation of an intermediate in the acid hydrolysis, whereas the neutral hydrolysis undergoes a concerted-type mechanism. There is a nice agreement between the characterized intermediate and available X-ray data and a good agreement with the kinetically estimated rate acceleration of hydrolysis with respect to analogous undistorted amide compounds. This work, along with previous ab initio calculations, describes a complex and rich chemistry for the hydrolysis of highly twisted amides as a function of pH. The theoretical data provided will allow for a better understanding of the available kinetic data of the rate acceleration of amides upon twisting and the relation of the observed rate acceleration with intrinsic differential reactivity upon loss of amide bond resonance.

Introduction

The hydrolysis reaction of amides, often used as a model for the cleavage of peptide bonds,[1,2] is central on a variety of biochemical processes. The water-promoted hydrolysis, or neutral hydrolysis, of nonactivated amides is very slow and in most cases undetectable.[3] The amide bond's stability is ascribed to its partial double bond character, caused by the resonance between the nitrogen lone pair and the π_{CO} bond.[4] As a consequence, amides show a characteristic short C−N bond length and a rigid planar conformation. A hypothesis for activation of amides toward hydrolysis establishes that the amide bond could be significantly weakened by twisting the amide bond in the reactant.[4,5] This twist would cause the breakdown of the $n_N \rightarrow \pi^*_{CO}$ resonance and leads to pyramidalization of the nitrogen and elongation of the C−N bond.[6] The twist of the amide bond could be induced by specific geometrical constraints in the reactants or by enzyme action on a preferential twisted conformation of the substrate. In fact, this type of "ground-state destabilization" has been suggested to be part of the mechanism of catalysis in the case of protein splicing.[7,8] This is as well the basis for the design of transition state analogues which are used as haptens to develop catalytic antibodies[9] that are able to catalyze peptide bond cleavage by inducing "ground-state destabilization" of the reactant.

Nonplanar deformations of amide bonds in peptides have been the focus of considerable interest.[10] For instance, X-ray data[11] and computational studies[12−17] on the rotational barrier of formamides and its derivatives support the idea of C−N bond weakening upon C−N bond twist. Unfortunately, little accurate kinetic data on hydrolysis of nonplanar twisted amides is available. However, in a seminal work by Blackburn et al., it was reported that the alkaline hydrolysis of benzoquinuclidin-2-one, a strained cyclic amide with a significantly twisted amide bond, was 10^7 times faster than its strainless counterpart.[18,19] This corresponds to a decrease in the reaction activation energy by about 10 kcal/mol. In agreement with these experiments, Brown et al. also reported[2,20] significant accelerations for the hydrolysis of distorted amides. Quite interestingly the degree of acceleration seems to depend on the pH conditions, ranging from 7 orders of magnitude for the alkaline hydrolysis to 11 orders of magnitude for acid-catalyzed hydrolysis. More recently, Kirby et al.[21−23] also reported the rapid hydrolysis in water (under slight acidic conditions) of a highly twisted amide bond in 1-aza-2-adamantanone, suggesting an even higher acceleration of the hydrolysis rate.

Computational studies[24−40] on the hydrolysis of amides have been mainly focused on the reaction of undistorted planar amides such as formamide. The specific question of how the twisting of the amides affects its properties was studied by Greenberg et al.[6,41] They found that in the gas phase and contrary to behavior of undistorted amides, *twisted amides are protonated at the nitrogen instead of at the oxygen*, which suggested *important mechanistic differences* for the hydrolysis of twisted amides in acidic and neutral medium. More recently we characterized[42] the pK_a in solution for a series of twisted amides, which confirmed the results of Greenberg et al., and revealed a pK_a of 6−7 for the most twisted amides. In two recent papers,[43,44] we made a comparative computational study of the alkaline and neutral hydrolysis of a twisted amide (**TA** in Figure 1) with respect to its planar analogue (**PA** in Figure 1), asserting a significant effect of the twist of the amide bond in the corresponding reaction barriers. In the alkaline hydrolysis,[43] the difference in energy barrier for the stepwise hydrolysis of these

* Corresponding author: xabier.lopez@ehu.es (X.L.)

10.1021/jp0604037 CCC: $33.50
Published on Web 07/11/2006

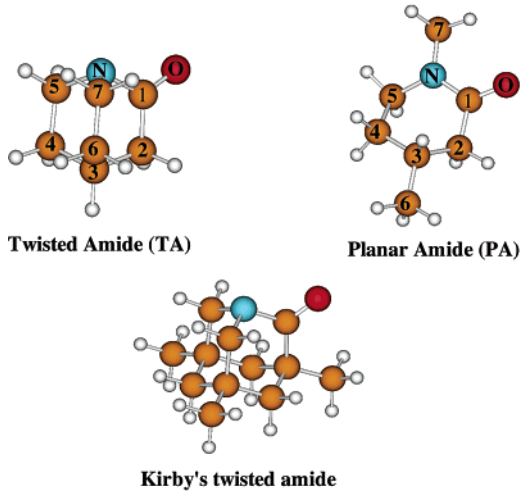

Figure 1. The two amide reactants used along the present study. On the left-hand side, the twisted amide is depicted (**TA**), and on the right-hand side the planar amide (**PA**).

two amides (Figure 1) was 7.0−9.7 kcal/mol. For the neutral hydrolysis,[44] we studied both a concerted and a stepwise mechanism with a second water molecule added which catalyzes the reaction by serving as a proton bridge, as considered by others.[29,30] We found that there is a preference for a concerted-type mechanism in the case of the hydrolysis of the highly twisted amides, due to the large proton affinity of the amide nitrogen. In addition, a substantial rate acceleration was found with respect to hydrolysis of the planar amide analogue **PA**.

In the present paper, we continue with this series of calculations, analyzing the acidic hydrolysis regime of a highly twisted amide and its analogous planar amide (see Figure 1). The comparative of the acidic hydrolysis (or H_3O^+-promoted hydrolysis) of a highly twisted amide versus its planar amide analogue is of added interest, since the difference in the protonation properties of amides upon twisting[6,41,42] suggests important mechanistic differences. Both the concerted and stepwise mechanism are considered, and the reaction is evaluated for the nonassisted and water-assisted mechanism. The calculations are carried out using the density functional theory in conjunction with a polarizable continuum model to take into account bulk solvent effects. This study complements our previous work in this field and allow us to characterize the similarities and differences in the hydrolysis of highly twisted amides at three different pH ranges: acid, neutral, and alkaline.

Methodology

Potential energy surfaces for the acidic hydrolysis of the twisted amide and its analogous planar amide (**TA** and **PA** in Figure 1) were characterized in the gas phase and in solution. All the calculations were carried out using the Gaussian 98 suite of programs.[45] Gas-phase structures were optimized at the B3LYP/6-31+G(d) level of theory. The electronic energy at these geometries were then refined by single-point calculations at the B3LYP/6-311++G(d,p) level of theory. The use of the B3LYP functional[46−49] is motivated by its overall reliability for similar problems[50] and, in particular, in the evaluation of reaction enthalphies for the hydrolysis of neutral amides.[31] The enthalpic and entropic corrections were determined with frequency calculations at the B3LYP/6-31+G(d) level of theory.[51] These frequencies were also used to verify the nature of the stationary points encountered along the potential energy surface. Thus, reactants, intermediates, and products showed real frequencies for all the normal modes of vibration, whereas transition states showed one imaginary frequency along the desired normal mode. The free energy was obtained as a sum of the B3LYP/6-311++G(d,p) energy and the zero-point vibrational energy (ZPVE), the vibrational correction to the ZPVE at 298 K, and the rotational and translational energies at 298 K. The zero-point vibrational energy and the thermal vibrational energy were calculated in the rigid rotor-harmonic oscillator approximation. The rotational and translational energies were treated classically as (1/2)*RT* per degree of freedom. Recent ab initio calculations have indicated that the rigid rotor-harmonic oscillator approximation[52] may lead to an overestimation of the entropic contribution to the activation free energies in hydrolysis reactions.[53] This is specially true for low-frequency modes[54] which can be best described as internal rotation modes. Although using a hindered rotor approximation or empirical corrections[54] will affect the absolute values of the activation barriers for the different reactions, it is not expected to affect significantly the relative activation free energies between analogous reactions, specially if small molecules with relative few degrees of freedom (like the ones presented here) are considered. Since the main purpose of this work is the determination of rate accelerations between analogous hydrolysis reactions of planar and twisted amides, these effects are predicted to be minor. However, it should be highlighted that an accurate determination of absolute free energy barriers for each reaction would probably require the need for further investigation using QM/MM simulation methods with converged sampling in an explicitly solvated environment.[55]

All structures were also optimized in solution using the self-consistent isodensity polarizable continuum model (SCI-PCM) method[56] at the B3LYP/6-31+G(d) level of theory, and the same level of theory was used for the frequency calculations. The value of the electron density used to describe the cavity's size and shape into which the solute will be placed was set to 0.0004 au, and 146 grid points were considered for the surface charges. It is expected that the biggest error in the evaluation of solvation free energies will be associated with the hydronium ion, since it also shows the highest solvation free energy in absolute value due to the combination of its small size and integral +1 charge. The experimental solvation free energy[57] for the hydronium ion is −104.0 kcal/mol, whereas our SCI-PCM value is of −108.3 kcal/mol. Thus an increase in the relative free energies in solution of around 4 kcal/mol is expected due to this error. However, notice that this will be irrelevant for the determination of relative barriers between the hydrolysis of the twisted and planar amides, since in both reactions we consider the same reference state.

The gas phase and solution energies were employed to calculate the relative energies with respect to the separate reactants: amide + H_3O^+ in the nonassisted reaction and amide + H_3O^+ + water in the water-assisted reaction. The relative energies are collected in Tables 2 and 4.

The nomenclature of the atoms in the various reaction mechanisms is summarized in Figure 2. The C_1 and O atoms correspond to the carbonyl atoms in the amide. The O_{nu} atom stands for the oxygen of the water molecule that makes the nucleophilic attack on the carbonyl C_1 atom. The proton that is being transferred from the nucleophile in the non-water-assisted mechanism is referred as H^1. On the other hand, when we have an additional water molecule in the hydrolysis mechanism, the oxygen atom of the water molecule that assists the hydrolysis is called O_{as}, and the H that is transferred from this water molecule to the other one is called H^1_{as}. In Figure 2, we

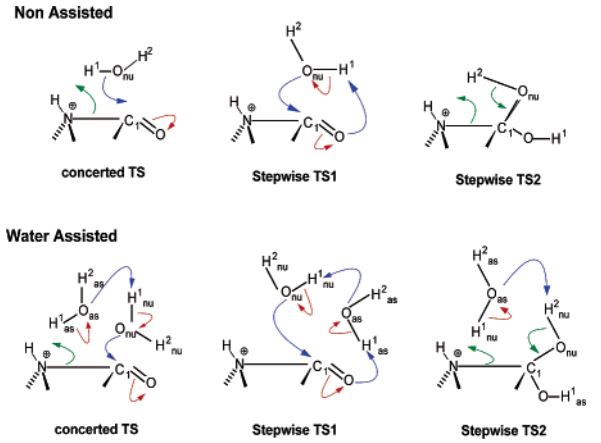

Figure 2. Nomenclature used in this paper for the relevant atoms in the transition states for the acid hydrolysis of the twisted N-protonated amide.

schematically show the atom nomenclature for some types of transition states.

The out-of-plane deformations are described by the angles τ, χ_C, and χ_N following the definitions of references.[11,58] The angle τ characterizes the mean twisting angle around the C_1-N bond and ranges from 0 (planar amide group) to 90 (when the two planes defined by the $O-C_1-C_2$ and C_5-N-C_7 atoms are perpendicular); χ_C and χ_N are measures of the degree of pyramidalization at the C_1 and N, respectively. They range approximately from 0 (planar sp^2 atoms) to 60 (tetrahedral sp^3 atoms). The four torsion angles $\omega_1 = O-C_1-N-C_5$, $\omega_2 = C_2-C_1-N-C_7$, $\omega_3 = C_2-C_1-N-C_5$, and $\omega_4 = O-C_1-N-C_7$, are combined to define the τ, χ_C, and χ_N as follows:

$$\tau = \frac{(\omega_1 + \omega_2)}{2}$$

$$\chi_C = \omega_1 - \omega_3 + \pi(\mathrm{mod}2\pi) = -\omega_2 + \omega_4 + \pi(\mathrm{mod}2\pi)$$

$$\chi_N = \omega_2 - \omega_3 + \pi(\mathrm{mod}2\pi) = -\omega_1 + \omega_4 + \pi(\mathrm{mod}2\pi)$$

The absolute values for these angles with projection on the 0−90 quadrant are found in Tables 1 and 3. In all cases, the oxygen atom used to calculate the ω_1 and ω_4 torsion angles corresponds to the original carbonyl oxygen rather than the water oxygen. For the product structures in which the amide bond is broken, these angles are of limited value. In those cases, we use the improper dihedrals, also indicated in those two tables.

Results

In this section we present the main structural and energetic features of the acidic hydrolysis of the twisted amide (**TA**). The structures were optimized both in gas phase and in solution (for more details see the Methodology section) although in the current section we only refer to the geometries optimized in solution. The reaction is studied following two different mechanisms: (i) The concerted mechanism shows only one transition state (TS) between the reactants and the product. (ii) The stepwise mechanism with a carbon tetrahedral intermediate and two transition states: the first one corresponds to a nucleophile attack of the water molecule at the carbonyl C_1 atom (TS1) of the protonated amide, and the second one to the cleavage of the amide bond (TS2). For both concerted and stepwise mechanisms, we also present the effect of an auxiliary water molecule which catalyzes the reaction by serving as a bridge in proton transfer.

To facilitate the identification of each transition state and intermediate of each reaction we will introduce a nomenclature to specify each stationary point. The subscripts c and s will specify whether the structure belongs to the concerted (c) or stepwise (s) mechanism. For example, $TS1_s$ will be used to name the first transition state in the stepwise mechanism and TS_c will refer to the transition state of the concerted mechanism. In addition, the superscript W will indicate the presence in the mechanism of an auxiliary water molecule which assists in the proton-transfer process. Thus, TS_c will correspond to the concerted transition state with no auxiliary water, whereas TS_c^W will name the concerted mechanism transition state with one auxiliary water molecule assisting the reaction.

(A) Nonassisted Hydrolysis. We consider the unprotonated amide and the hydronium ion as the reactants of the reaction. This will facilitate the comparison with our previous work[43,44] for the alkaline and neutral hydrolysis, in which obviously the reference amide was in its unprotonated form. The unprotonated twisted amide presents an amide bond with a significant degree of twist, which is enforced by the cage strain imparted by the molecular structure. The twist measured by the τ angle is 89.9°, which is almost a 100% degree of twist. Due to this twist, the carbonyl π_{C_1-O} orbital and the nitrogen's lone pair lie in a perpendicular plane, and therefore, the $n_N \rightarrow \pi^*_{C_1-O}$ resonance of untwisted amide bonds is prevented in this case. This leads to the loss of the partial double bond character of the C_1-N bond, in particular, the length of this bond in TA is 1.448 Å, almost 0.1 Å longer than the one found in formamide at the same level of theory.

It is well established that the initial protonation of the amide by the hydronium ion leads to the N-protonated tautomer.[6,41,42] In fact, highly twisted amides can show very high pK_a values (5−7),[42] which indicates that the possibility that the hydrolysis of highly twisted amides goes through an acid-type reaction is available at significant higher pH values than for undistorted amides. In the protonated twisted amide (TA_H), the amide bond is highly activated and the C_1-N bond distance is 1.529 Å, 0.1 Å larger than that in the unprotonated TA amide.[59] Concomitantly, the C_1-O distance is 1.189 Å, 0.3 Å shorter. As expected, the protonation does not change the maximum degree of the twisting (τ is 90.0), the planarity of the C_1 atom (χ_C is 0.0), and the pyramidalization of the N atom (χ_N is 59.1).

(1) Concerted Mechanism. (a) Structures. The reaction pathway is depicted in Figure 3 and the geometrical parameters are presented in Table 1. The unique transition state of this reaction pathway corresponds to the nucleophilic attack of the O_{nu} at the carbonyl C_1 atom, concerted with a proton transfer from the water molecule to the nitrogen atom and the cleavage of the peptide bond. All these changes do not occur simultaneously. If we look at the geometry of the TS_c and based on the IRC pathway, we see that the nucleophilic attack is advanced (the $O_{nu}-C_1$ distance is 1.638 Å), and the C_1-N bond is almost broken (2.603 Å), although the proton is not transferred yet since this atom is much closer to O_{nu} than to the N atom (0.989 and 2.250 Å, respectively). The early formation of the C_1-O_{nu} bond is also reflected in the conformation of the C_1 atom that has lost its planarity (the χ_C value is 44.0°).

In the characterized product of the reaction, the amide bond is completely broken (the C_1-N distance is 3.532 Å) and a carboxyl group is formed with a C_1-O_{nu} distance of 1.341 Å. Notice that the proton is fully transferred to the nitrogen (the $N-H^1$ and $O_{nu}-H^1$ distances are 1.033 and 4.056 Å, respectively). Besides, one of the protons bound to nitrogen is hydrogen bonded to the unprotonated oxygen of the carboxylic

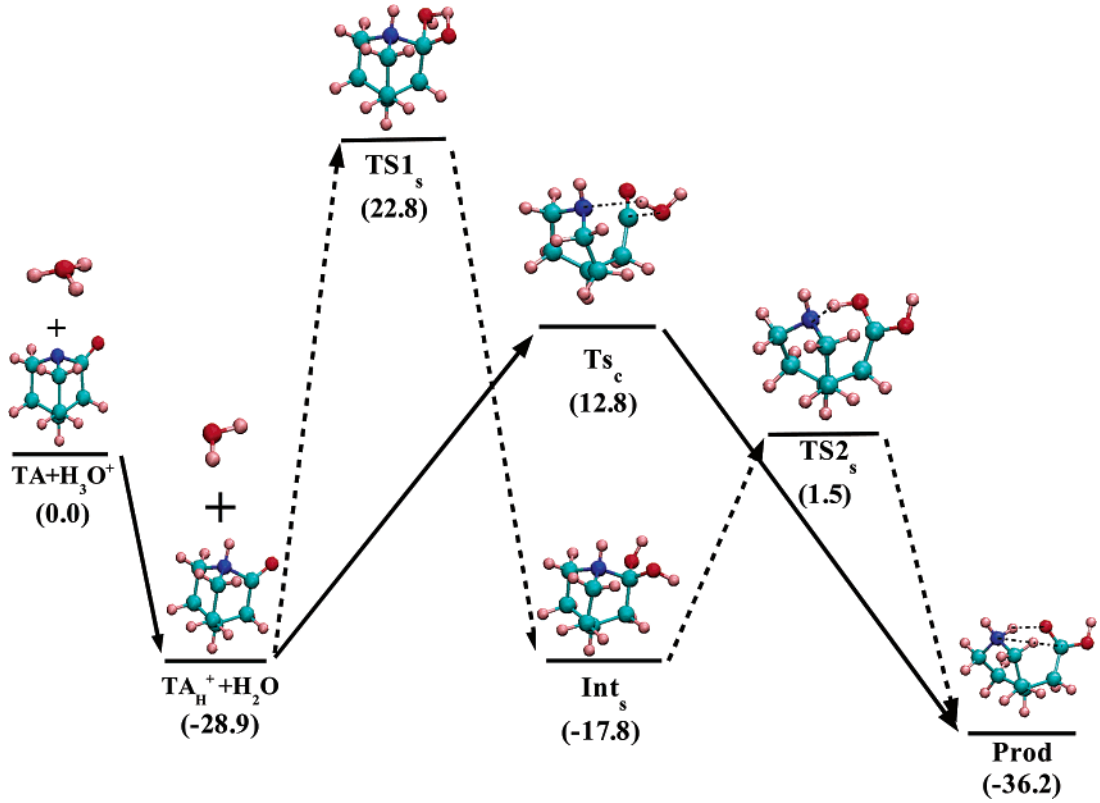

Figure 3. The B3LYP/6-31+G(d) structures for the twisted amide in the nonassisted hydrolysis reaction for both the concerted (regular line) and stepwise (dashed line) mechanism. The values correspond to the relative free energy (ΔG) in kcal/mol for structures optimized in solution. Note that the PES values are not scaled.

TABLE 1: B3LYP/6-31+G* Geometrical Parameters for the Stationary Points of the PES Values of the Nonassisted Acidic Hydrolysis of Twisted Amide following the Concerted and Stepwise Mechanisms[a]

Concerted Mechanism

	bond distances					angles			improper dihedral	
	C_1-N	C_1-O	C_1-O_{nu}	H^1-O_{nu}	H^1-N	τ	χ_c	χ_n	dh_C	dh_N
TA	1.453	1.209				89.4	0.1	62.4	180.0	117.2
	1.448	**1.216**				**89.9**	**0.0**	**62.8**	**180.0**	**116.7**
TA_H	1.553	1.189				90.0	0.0	58.0	180	120.9
	1.529	**1.189**				**90.0**	**0.1**	**59.1**	**179.9**	**120.1**
HB	1.532	1.193	3.568	0.970	3.569	90.0	0.0	58.5	180	120.4
	1.516	**1.198**	**3.647**	**0.971**	**3.445**	**89.3**	**0.1**	**59.1**	**179.9**	**120.2**
TS_c	2.648	1.146	2.020	0.981	2.137	56.6	27.1	69.1	152.9	115.4
	2.603	**1.172**	**1.638**	**0.989**	**2.250**	**57.0**	**44.0**	**63.0**	**135.9**	**116.6**
Prod	3.455	1.229	1.332	3.888	1.044	87.4	9.0	67.7	179.2	116.1
	3.532	1.224	1.341	4.056	1.033	86.5	11.3	67.8	178.9	117.5

Stepwise Mechanism

	bond distances							angles			improper dihedral	
	C_1-N	C_1-O	C_1-O_{nu}	H^1-O_{nu}	H^1-O	H^2-O_{nu}	H^2-N	τ	χ_c	χ_n	dh_C	dh_N
$TS1_s$	1.564	1.291	1.633	1.193	1.348	0.980	3.247	28.1	40.4	57.3	139.7	120.3
	1.559	**1.309**	**1.568**	**1.184**	**1.365**	**0.984**	**3.224**	**18.8**	**42.5**	**58.5**	**137.4**	**120.2**
Int_s	1.561	1.392	1.383	2.671	0.974	0.975	2.775	23.5	56.7	57.3	126.3	123.3
	1.557	**1.390**	**1.384**	**2.635**	**0.975**	**0.977**	**2.725**	**28.1**	**57.9**	**57.4**	**122.3**	**123.3**
$TS2_s$	2.914	1.290	1.292	2.242	0.983	0.980	2.560	49.2	60.5	68.3	171.0	121.6
	3.019	**1.286**	**1.286**	**2.264**	**0.987**	**0.981**	**2.793**	**51.1**	**60.2**	**68.0**	**173.2**	**123.7**

[a] The bond distances are in Å and the angles and improper dihedrals in degrees for the structures optimized in gas-phase and in solution (in bold).

group. Because of the cleavage of the amide bond, τ, χ_C, and χ_N angles have lost their meaning and in order to get useful information on the conformation of atoms around the nitrogen and carbon atoms, it is more appropriate to analyze the values of the improper dihedrals. In this sense, it can be observed that the C_1 atom has recovered its planarity (dh_C is 178.9°) and the nitrogen has adopted a pyramidal conformation (dh_N is 117.5°).

(b) Energy Profile. The relative energies for the different stationary points of this reaction pathway are presented in Table 2 for the geometries optimized in gas phase and in solution. The relative energies are separated in their different contributions. In gas phase, all the electronic energies are negative due to high stabilization caused by the proton transfer from hydronium to the amide (−64.4 kcal/mol). Inclusion of ZPVE

TABLE 2: Relative Electronic Energies (ΔE_e), Zero-Point Energies (ΔE_0), Enthalpies (ΔH), Entropic Contributions ($T\cdot\Delta S$) and Free Energies (ΔG) for the Stationary Points Involved in the Nonassisted Acidic Hydrolysis Reaction of the Twisted Amide in Gas Phase and in Solution (Values Presented in Bold)

	ΔE_e	ΔE_0	ΔH	$T\cdot\Delta S$	ΔG
			Concerted Mechanism		
$TA + H_3O^+$	0.0	0.0	0.0	0.0	0.0
	0.0	**0.0**	**0.0**	**0.0**	**0.0**
$TA_H^+ + H_2O$	−64.4	−63.4	−63.4	−1.3	−62.1
	−31.2	**−30.2**	**−30.2**	**−1.3**	**−28.9**
HB	−80.4	−78.0	−77.9	−8.7	−69.2
	−38.0	**−36.3**	**−36.5**	**−8.6**	**−27.9**
TS_c	−43.0	−41.1	−41.9	−11.6	−30.3
	0.2	**2.1**	**1.3**	**−11.5**	**12.8**
Prod	−92.2	−86.6	−87.6	−11.7	−75.9
	−52.0	**−46.6**	**−47.6**	**−11.4**	**−36.2**
			Stepwise Mechanism		
$TS1_s$	−28.4	−26.8	−28.4	−13.0	−15.3
	9.2	**10.9**	**9.3**	**−13.6**	**22.8**
Int_s	−74.1	−68.6	−70.1	−13.1	−57.0
	−34.2	**−29.0**	**−30.5**	**−12.7**	**−17.8**
$TS2_s$	−52.2	−48.6	−49.9	−12.5	−37.4
	−12.3	**−9.5**	**−10.7**	**−12.3**	**1.5**

corrections increases the relative energies between 1 and 5 kcal/mol. Entropic contributions also increase the relative energy of the species with respect to reactants because of the loss of translational and rotational degrees of freedom when rearranging from two infinitely separated reactants into one single molecular structure. Accordingly, in the gas phase the reaction is exothermic with a ΔH_{gas} of −87.6 kcal/mol and a free energy barrier of −30.3 kcal/mol.

Bulk solvent effects favor the separated reactants and specially the reactants that combine charge with a small volume, i.e., the hydronium ion. As a consequence, there is a substantial increase of relative energies of all the species with respect to the unprotonated amide plus hydronium molecule, although the energy profile is analogous to the gas phase. The reaction is still very exothermic with a reaction enthalpy of −47.6 kcal/mol and a free energy barrier of 12.8 kcal/mol.

(2) Stepwise Mechanism. In the stepwise mechanism the hydrolysis reaction takes place in two steps (apart from the initial amide protonation step): (i) the nucleophilic attack of the water molecule at the carbonyl C_1 atom concerted with a proton transfer from the water molecule to the oxygen atom forming a tetrahedral intermediate and (ii) the cleavage of the C_1-N peptide bond concerted with a proton transfer from one of the oxygens to the nitrogen atom. The reaction pathway is depicted in Figure 3.

(a) Structures. Selected geometrical parameters are shown in Table 1. The reactant and the product are the same than in the concerted mechanism. The first transition state ($TS1_s$) corresponds to the nucleophilic attack of the O_{nu} water oxygen atom on the carbonyl group concerted with a proton transfer from the water molecule to the carbonyl oxygen. The C_1-O_{nu} bond distance is 1.568 Å, slightly shorter than that in the concerted mechanism (1.638 Å). The nucleophilic attack changes the conformation of the C_1 atom adopting a nonplanar conformation (χ_C is 42.5). The H^1 is transferred from the water molecule to the carbonyl oxygen, and at $TS1_s$ the proton is shared by both atoms, although it is slightly closer to O_{nu} (1.184 Å) than to the carbonyl O atom (1.365 Å). The C_1-N amide bond is only slightly elongated by 0.03 Å at $TS1_s$ with respect to the amide bond in protonated amide.

At intermediate Int_s, the proton transfer is completed ($O-H^1$ is 0.975 Å) and the C_1 atom is bound to two oxygen atoms with similar distances (1.390 and 1.384 Å) and in a tetrahedral conformation. The amide bond distance is still very similar, 1.557 Å, to the one shown by the protonated amide, 1.529 Å. Kirby et al. characterized[22] by X-ray diffraction the tetrahedral intermediate in the hydrolysis reaction of a highly twisted amide similar to our TA (illustrated in Figure 1). There is a very nice agreement of our structure with the X-ray structure for the intermediate of Kirby: They determined a peptide bond distance of 1.552(4) Å and the distance in our optimized structure is 1.557 Å, in addition, the two C−O bond distances for their structure were 1.382(4) Å, while the distances in our tetrahedral intermediate are 1.384 and 1.390 Å. This suggests that the intermediate trapped by Kirby et al. corresponded to the intermediate of the acid hydrolysis reaction (see Discussion section).

The second step of the reaction is the cleavage of the amide bond concerted with a proton transfer from one of the oxygens to the nitrogen atom. The transferred proton is the one bound to the O_{nu} atom (H^2). The bond breaking/forming processes are not synchronous. At the $TS2_s$ transition state, the proton transfer is at a very early stage (the H^2-O_{nu} distance is 0.981 Å) while the amide cleavage is quite advanced (the C_1-N distance is broken 3.019 Å).

(b) Energy Profile. The relative energies for this reaction are presented in Table 2. The reactant and the product are the result of the same concerted mechanism so the reaction is exothermic both in gas phase and in solution. The relative free energies in the gas phase of $TS1_s$ and $TS2_s$ are −15.3 and −37.4 kcal/mol, respectively, so the first step is clearly rate limiting. When solvent effects are considered, both barriers increased to 22.8 kcal/mol ($TS1_s$) and 1.5 kcal/mol ($TS2_s$), but still the first step is the clear rate-limiting step. The relative free energy of the intermediate is −57.0 kcal/mol in the gas phase and −17.8 in solution. Thus, the barrier for intermediate cleavage is around 19.3 kcal/mol in solution, a sufficiently high barrier to have a significant lifetime to be detected.

(B) Water-Assisted Hydrolysis. In this type of mechanism, the reaction is catalyzed by an extra water molecule which assists in the proton-transfer processes along the reaction. The reference reactants for this reaction are the unprotonated amide, an hydronium ion, and a water molecule. After the protonation of the amide TA_H, we have two independent water molecules, one of them acts as the nucleophile whereas the other is the assistant water molecule serving as a bridge in proton transfers. Along the reaction pathway there are two different protons that are transferred (H_{nu}^1 and H^1_{as}) which are defined in Figure 2. This section is subdivided analogously to the previous section, first we discuss the concerted mechanism, and then the stepwise mechanism. Besides, in each case we first present the structures and then the energies. A diagram showing the final free energies for each stationary point of both pathways can be found in Figure 4.

(1) Concerted Mechanism. (a) Structures. Selected geometrical parameters can be found in Table 3. The reactant structures are the same as those in the nonassisted reaction, so we do not describe them in this section. Several attempts to optimize the geometries of TS_c^W and $Prod^W$ with the SCI-PCM algorithm failed, so their geometries correspond to gas-phase optimizations. Bulk solvent effects for these structures were determined by single-point calculations at the gas-phase geometries. The error due to this fact is expected to be small because gas-phase and solution geometries are in general very similar for the rest of mechanisms characterized in this paper.

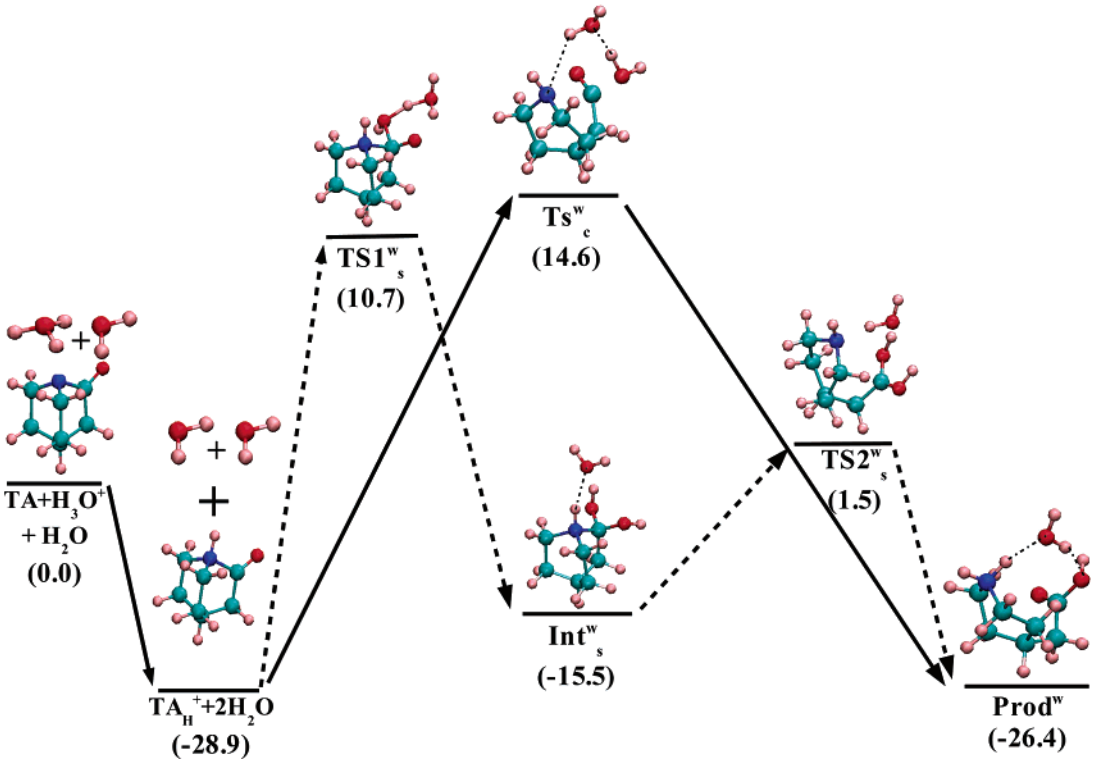

Figure 4. The B3LYP/6-31+G(d) structures for the twisted amide in the water-assisted hydrolysis reaction for both the concerted (regular line) and stepwise (dashed line) mechanism. The values correspond to the relative free energy (ΔG) in kcal/mol for structures optimized in solution. Note that the PES values are not scaled. See Figure 5 for a scaled profile.

TABLE 3: B3LYP/6-31+G* Geometrical Parameters for the Stationary Points of the PES Values of the Water-Assisted Acidic Hydrolysis of Twisted Amide following the Concerted and Stepwise Mechanisms.

Concerted Mechanism

	bond distances							angles			improper dihedral	
	C_1-N	C_1-O	C_1-O_{nu}	$H_{nu}^1-O_{nu}$	$H_{nu}^1-O_{as}$	$H^1_{as}-O_{as}$	$H^1_{as}-N$	τ	χ_c	χ_n	dh_C	dh_N
TA	1.453	1.209						89.4	0.1	62.4	180.0	117.2
	1.448	**1.216**						**89.9**	**0.0**	**62.8**	**180.0**	**116.7**
TA_H	1.553	1.189						90.0	0.0	58.0	180	120.9
	1.529	**1.189**						**90.0**	**0.1**	**59.1**	**179.9**	**120.1**
TS_c^W	2.905	1.161	1.731	1.039	1.513	0.973	2.554	32.4	39.1	69.3	174.2	117.7
$Prod^W$	4.046	1.375	1.210	3.735	0.976	1.785	1.042	86.9	65.5	58.7	180.0	119.3

Stepwise Mechanism

	bond distances										angles			improper dihedral	
	C_1-N	C_1-O	C_1-O_{nu}	$H_{nu}^1-O_{nu}$	$H_{nu}^1-O_{as}$	H_{nu}^1-N	$H_{nu}^2-O_{nu}$	$H_{nu}^2-O_{as}$	$H^1_{as}-O_{as}$	$H^1_{as}-O$	t	χ_c	χ_n	dh_C	dh_N
$TS1_s^W$	1.619	1.260	1.626	1.310	1.143	3.382	0.974	2.959	1.021	1.640	35.4	47.4	57.6	132.6	120.4
	1.631	**1.267**	**1.583**	**1.280**	**1.166**	**2.971**	**0.978**	**2.912**	**1.013**	**1.713**	**36.8**	**48.7**	**59.1**	**131.2**	**120.0**
Int_s^W	1.557	1.402	1.375	3.408	0.973	3.463	0.982	2.013	3.762	0.973	33.2	58.3	42.3	121.7	123.4
	1.555	**1.397**	**1.380**	**3.414**	**0.973**	**3.516**	**0.987**	**1.886**	**3.830**	**0.975**	**33.0**	**58.6**	**58.0**	**121.4**	**123.3**
$TS2_s^W$	3.381	1.305	1.274	2.656	1.051	1.646	1.072	1.436	2.213	0.984	40.8	62.5	68.8	173.7	116.9
	3.040	**1.290**	**1.286**	**2.764**	**0.984**	**2.184**	**1.010**	**1.697**	**1.823**	**0.999**	**34.2**	**61.4**	**69.4**	**178.5**	**116.6**
$Prod^W$	4.046	1.375	1.210	4.313	1.785	1.042	3.735	0.976	3.228	0.980	86.9	65.5	58.7	180.0	119.3

[a] The bond distances are in Å and the angles and improper dihedrals in degrees for the structures optimized in gas phase and in solution (in bold).

The transition state of the water-assisted concerted mechanism TS_c^W shows a quite advanced nucleophilic attack with a C_1-O_{nu} distance of 1.731 Å, the cleavage of the C_1-N bond is also quite accomplished at the transition state (C_1-N distance is 2.905 Å), but the protons are not transferred yet. The H_{nu}^1 atom is closer to the O_{nu} atom (1.039 Å) than to the O_{as} atom (1.513 Å) and the H^1_{as} atom is still bound to the O_{as} (0.973 Å). The C_1-N distance is 0.3 Å longer than in the nonassisted TS_c and the C_1-O_{nu} distance is longer as well but by only 0.1 Å.

The product of the reaction is analogous to that of the nonassisted reaction, the main difference being that the C_1-N distance is 0.5 Å longer than in the nonassisted case, i.e., 4.046 Å. This is due to the presence of the additional water molecule, which forms two hydrogen bonds, one with the amine and the other with the carboxylic group.

(b) Energy Profile. Relative energies for the different structures of the water-assisted mechanism can be found in Table 4. The reference reactants for the calculation of relative energies are the twisted amide, the hydronium ion, and a water molecule. The fact that as reference state we have three infinitely separated

TABLE 4: Relative Electronic Energies (ΔE_e), Zero-Point Energies (ΔE_0), Enthalpies (ΔH), Entropic Contributions ($T\cdot\Delta S$), and Free Energies (ΔG) for the Stationary Points Involved in the Water-Assisted Acidic Hydrolysis Reaction of the Twisted Amide in Gas Phase and in Solution (values presented in bold)[a]

	ΔE_e	ΔE_0	ΔH	$T\cdot\Delta S$	ΔG
	Concerted Mechanism				
$TA + H_3O^+ + H_2O$	0.0	0.0	0.0	0.0	0.0
	0.0	**0.0**	**0.0**	**0.0**	**0.0**
$TA_H{}^+ + 2(H_2O)$	−64.4	−63.4	−63.4	−1.3	−62.1
	−31.2	**−30.2**	**−30.2**	**−1.3**	**−28.9**
HB	−88.0	−82.9	−83.6	−18.5	−65.0
	−41.1	**−37.2**	**−38.5**	**−19.8**	**−18.7**
TS_c^W	−53.1	−49.1	−50.4	−20.5	−29.9
			−5.9[b]		**14.6**[b]
Prod	−96.4	−88.6	−90.0	−20.2	−69.8
			−47.0[b]		**−26.8**[b]
	Stepwise Mechanism				
$TS1_s^W$	−60.7	−55.5	−58.3	−24.0	−34.3
	−15.3	**−10.6**	**−13.5**	**−24.2**	**10.7**
Int_s^W	−90.5	−82.4	−84.5	−22.7	−61.8
	−42.3	**−35.2**	**−37.1**	**−21.6**	**−15.5**
$TS2_s^W$	−74.0	−68.4	−71.0	−23.9	−47.1
	−24.8	**−19.1**	**−21.3**	**−22.8**	**1.5**

[a] The reference was chosen as $A + (H_3O^+) + (H_2O)$. [b] Geometries optimized in gas phase.

reactants make the entropic contributions to increase significantly the relative energies of the transition state and product with respect to the reactants, by around 20 kcal/mol. This is due to the loss of the rotational and translational entropy. As a consequence, when looking at the gas-phase enthalpic barrier we can state a significant catalytic effect of the assistant water molecule. Thus the relative energy of TS_c^W is −50.4 kcal/mol, lower than the energy of the nonassisted TS_c, −41.9 kcal/mol. However, if we look at the relative free energies now the numbers are more similar, −29.9 kcal/mol for TS_c^W and −30.3 kcal/mol for TS_c.

The inclusion of the bulk solvent effect again favors the separated reactants, and hence, higher relative energies are obtained. We emphasized, however, that in this case these bulk solvent effects have been evaluated at the gas-phase geometries, and therefore they are less reliable. The final aqueous free energy barrier for the reaction is 14.6 kcal/mol, and the reaction free energy is −26.8 kcal/mol.

(2) Stepwise Mechanism. In the stepwise mechanism, the auxiliary water molecule acts as a bridge in proton transfer in both steps of the reaction. A scheme with the nomenclature for the transferred protons can be found in Figure 2. There are two protons that are transferred along the reaction pathway: (i) $H_{nu}{}^1$ is initially located at the nucleophilic water molecule, in the first step this proton goes to the assistant water molecule whereas in the second step it goes to the nitrogen; (ii) $H^1{}_{as}$ initially is located at the assistant water molecule, in the intermediate is bound to the carbonyl oxygen and in the second step it returns back to the assistant water molecule.

(a) Structures. The structures optimized in solution with the SCI-PCM algorithm are shown in Figure 4 and selected geometrical parameters can be found in Table 3. For this pathway, we were able to optimize all the structures with the SCI-PCM method, and we will comment only on these geometries throughout the text below. The first step corresponds to the nucleophilic attack of O_{nu} on the carbonyl group and a proton transfer to the oxygen atom of the carbonyl group. $TS1_s^W$ is the transition state for this first step, which shows a $O_{nu}-C_1$ distance of 1.583 Å very similar to the one in the nonassisted $TS1_s$ (1.568 Å), and 0.2 Å shorter than in the concerted TS_c^W transition state. Therefore, at the transition state the nucleophilic attack is more advanced than in the concerted mechanism with little influence of the assistant water molecule in this behavior. The $H_{nu}{}^1$ proton is located at very similar distances from O_{nu} (1.280 Å) and O_{as} (1.166 Å); however, the $H^1{}_{as}$ proton transfer is still at an early stage, being $H^1{}_{as}-O_{as}$ distance 1.013 Å. Finally the amide C_1-N bond distance is 1.631 Å, 0.072 Å longer than that in the nonassisted case.

The structure of the intermediate in the water-assisted mechanism Int_s^W is very similar to the intermediate Int_s of the nonassisted case. The difference between both structures is that in Int_s^W there is a water molecule hydrogen bound to the proton of the nitrogen. The bond distances of the nearby atoms to the carbon and to the nitrogen are very similar in both cases. The C_1 atom presents the typical tetrahedral conformation (χ_C is 58.6) for the intermediate of the reaction, and the C_1-N bond distance is 1.555 Å, only slightly elongated (by around 0.02 Å) with respect to the protonated amide reactant. As in the nonassisted reaction, we note the coincidence between the geometrical parameters for our optimized intermediate and the characterized geometrical data by X-ray diffraction (amide bond distance of 1.552(4) Å and C−O bond distances were 1.382(4) Å).

The transition state for the second step of the reaction, $TS2_s^W$, shows a quite long C_1-N distance, namely 3.040 Å slightly longer than in the nonassisted $TS2_s$, 3.019 Å and around 0.1 Å larger than in the concerted TS_c^W. However, the degree of proton transfer is low, since $H_{nu}{}^1$ and $H^1{}_{as}$ protons are still bound to O_{as} and O, respectively. The $H_{nu}{}^1$ proton is at 0.984 and 2.184 Å with respect to O_{as} and N, respectively, whereas $H_{nu}{}^2$ is at 1.010 and 1.697 Å with respect to O_{nu} and O_{as}. Therefore, there is a high asynchrony in the second step of the reaction between amide bond cleavage and proton transfer, the former occurring first than the latter.

(b) Energy Profile. Relative energies are summarized in Table 4. As in the nonassisted case, the first step of the reaction, $TS1_s^W$, is the rate-limiting step; however, the effect of the assistant water molecule in relaxing the corresponding barriers is more important than that for the concerted mechanism. In the gas phase, the ΔH of $TS1_s^W$ is −58.3 kcal/mol, 29.9 kcal/mol lower than in the nonassisted reaction, whereas ΔG is −34.3 kcal/mol, 19.0 kcal/mol lower than in the nonassisted reaction. On the other hand, the ΔG of TS2 is −47.1 kcal/mol, almost 10 kcal/mol lower than the nonassisted TS2.

Bulk solvent effects again favor the separated reactants although the effect is not the same at both transition states. The solvation free energy for $TS1_s^W$ is higher (in absolute value) than that for $TS2_s^W$. Nevertheless, the first step of the reaction is still rate limiting with a free energy barrier of 10.7 kcal/mol versus the 1.5 kcal/mol relative free energy displayed by $TS2_s^W$. Also, comparing these numbers with the values obtained for the concerted mechanism, we can conclude that the relative free energies and enthalpies for the transition states of the stepwise mechanism are lower than the barrier obtained for the transition state of the concerted mechanism (ΔG of TS_c^W was 14.6 kcal/mol); therefore, we can say that the water-assisted stepwise mechanism is the preferred pathway for the acidic hydrolysis of the highly twisted amide **TA**. This implies the formation of an intermediate structure with a sufficiently long lifetime to be detected, since the difference in free energy between this intermediate and $TS2_s^W$ is 17.0 kcal/mol.

TABLE 5: Relative Electronic Energies (ΔE_e), Zero-Point Energies (ΔE_0), Enthalpies (ΔH), Entropic Contributions ($T\cdot\Delta S$), and Free Energies (ΔG) for the Stationary Points Involved in the Acidic Hydrolysis Reaction of the Planar Amide in Gas Phase and in Solution (values presented in bold),

	ΔE_e	ΔE_0	ΔH	$T\cdot\Delta S$	ΔG
	Nonassisted				
$PA_H^+ + H_2O$	−57.8	−57.7	−57.6	−0.7	−56.9
	−21.0	**−21.1**	**−21.0**	**−0.8**	**−20.2**
HB	−77.1	−75.2	−75.4	−9.1	−66.3
TS1	−13.6	−13.1	−14.7	−13.1	−1.6
	26.7	**26.9**	**25.3**	**−13.0**	**38.3**
Int	−48.2	−43.9	−45.3	−12.5	−32.8
	−7.7	**−3.4**	**−4.8**	**−12.4**	**7.7**
TS2	−27.0	−24.3	−25.6	−12.0	−13.6
	10.6	12.9	11.7	−11.4	23.1
Prod	−64.9	−60.4	−61.3	−10.8	−50.5
	−26.9	**−22.3**	**−23.3**	**−11.1**	**−12.2**
	Water Assisted				
$PA_H^+ + + H_3O^+ + H_2O$	0.0	0.0	0.0	0.0	0.0
	0.0	**0.0**	**0.0**	**0.0**	**0.0**
$PA_H^+ + 2(H_2O)$	−57.8	−57.7	−57.6	−0.7	−56.9
	−21.0	**−21.1**	**−21.0**	**−0.8**	**−20.2**
$TS1^W$	−34.7	−31.2	−34.0	−23.8	−10.2
	10.2	**14.0**	**11.2**	**−24.0**	**35.2**
Int^W	−61.3	−55.0	−56.6	−20.9	−35.7
	−13.9	**−8.0**	**−9.6**	**−21.1**	**11.5**
$TS2^W$	−52.2	−48.0	−50.5	−23.1	−27.5
			−1.4[b]		**21.7**[b]
$Prod^W$	−77.5	−70.9	−72.2	−19.6	−52.6
			−24.9[b]		**−5.3**[b]

[a] For both nonassisted and water-assisted reaction pathways. [b] Geometries optimized in gas phase.

Planar Amide as Reference. To determine the rate acceleration of the acidic hydrolysis caused by the twist of the amide bond, the same methods as in the previous section were employed to characterize barriers for the acidic hydrolysis of an undistorted planar amide **PA** (see Figure 1) closely related to the highly twisted amide **TA**, which comes from the hydrogenation and cleavage of the **TA** C_6-C_7 bond. This leads to the breaking of the cage structure relaxing the geometrical constraints that maintained the amide bond in a twisted conformation. The **PA** reactant now shows a planar untwisted amide bond with a corresponding low value of τ, 1.8°, and a nitrogen atom in a quasi-planar conformation ($\chi_N = 8.4°$). This is the standard situation for an undistorted amide bond with some degree of delocalization between the lone pair of the nitrogen and carbonyl π bond, leading to a partial double C_1-N bond character. In fact, the C_1-N bond length is shorter, 1.363 Å, than that for the twisted amide reactant, 1.448 Å. An important difference in the acid hydrolysis of planar and twisted amides is that the protonation of the planar amide reactant occurs at the oxygen, and therefore, we have a different mechanism for the acid hydrolysis compared to the one previously described for the twisted amide. In addition, the O-protonation makes the concerted mechanism very unlikely, since it would require a double proton transfer to the nitrogen atom in an unique step. Therefore, only a stepwise mechanism was considered in this case.

The energetic values are presented in Table 5. Due to presence of the methyl group at the C_3 position there are two possibilities for the reaction, which correspond to attacks and proton transfers in an exo or an endo position with respect to this methyl group. However, as shown definitely in the neutral hydrolysis,[44] the endo attack is a more stable pathway. Hence, we discuss only this reaction pathway.

The energetic barriers are higher than the barriers of the twisted amide. In the gas phase all the relative energies (electronic, enthalpic, free energy) are negative with respect to the unprotonated amide and water reactants due to the high energy relaxation upon amide protonation. The inclusion of solvent effects lead to higher relative energies, and now the transition states and intermediate show positive relative free energies. The first step of the reaction is the rate-limiting step with a free energy barrier of 38.3 kcal/mol in the nonassisted mechanism and 35.2 in the water-assisted mechanism.

Comparisons with the available experimental data and theoretical calculations on acidic hydrolysis are not free of difficulties due to the different amide reactants and reference states used in theoretical calculations when evaluating relative energies. Experimentally, Guthrie et al.[60] reported an activation free energy for DMF of 26.3 kcal/mol at 25 °C, while Langlois and Broche[61] determined an activation energy of 18.4 kcal/mol for the same undistorted amide. Besides, Bolton and coworkers[62,63] measured the acidic hydrolysis for a large set of primary amides. They found that the activation energy was in the range of 18.8−21.5 kcal/mol. More recently, the group of Brown[64] reported the study of the formamide hydrolysis and they estimated a ΔH of 17.0 ± 0.4 kcal/mol for the acidic hydrolysis. These values for enthalpic and free energy barriers are significantly smaller than the ones characterized in the present work for planar amide **PA**, which shows an enthalpic barrier of 32.2 kcal/mol and free energy barrier of 55.4 kcal/mol with respect to the protonated amide plus two water molecules infinitely separated.

On the other hand, most of the theoretical studies for the acid hydrolysis of amides are based in formamide as amide reactant. Krug et al.[27] determined the acidic hydrolysis for the formamide in gas phase taken into account both the N- and O- protonation state at the MP2/6-31G**//4-31G level of theory, where they obtained an electronic energy barrier of 24.0 kcal/mol for the O-protonated case, the analogous pathway to our planar amide, choosing the protonated amide and separately water molecules as reference. On the other hand, Antonczak et al.[29,30] used as reference the hydrogen-bonded structure between formamide and a water molecule, plus another water molecule infinitely separated that acted as the nucleophile of the reaction. They obtained an electronic energy barrier of 27.6 and −6.9 kcal/mol for the nonassisted and water-assisted reaction respectively, at MP2/6-31G**//B3LYP/6-31G** level of theory in gas phase. Manojkumar et al.[65] calculated an electronic barrier of 24.5 kcal/mol using the same reference for the acidic hydrolysis of formamide at MP2/6-311++G**//B3LYP/6-311++G**. Since, these values were lower than the barrier characterized for **PA**, we calculated the energy barriers for TS1 of both formamide and *N*,*N*-dimethylacetamide (DMA) using the same protocol described in the Methodology section, considering both the nonassisted and water-assisted pathway. The departing structure for the optimization was "equivalent" to the TS1 of PA, where we kept the same geometrical disposition for the water molecules(s) and the amide bond, changing in each case the side chain for the formamide and *N*,*N*-dimethylacetamide. In the case of the formamide, we obtained an electronic barrier of 29.2 kcal/mol for the nonassisted reaction and −4.6 kcal/mol for the water-assisted reaction, in good agreement with the results presented by Antonczak et al.[29,30] On the other hand, the electronic barrier of DMA was found to be 40.3 kcal/mol in the nonassisted reaction and 15.3 kcal/mol in the water-assisted one, clearly closer to the barrier of **PA** (44.2 and 23.1 kcal/mol, respectively) than to the formamide's. On the basis of these

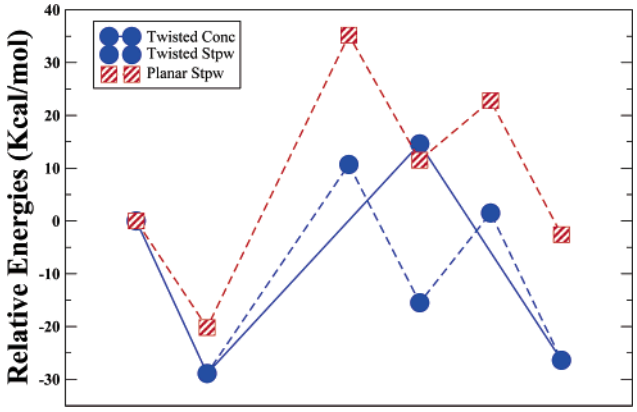

Figure 5. Aqueous free energy reaction profiles (see Methodology) comparing the water-assisted hydrolysis reaction through a concerted and a stepwise mechanism between the twisted and planar amides.

results, we can conclude that our methodology is appropriate and that it is coherent with previous ab initio calculations. The higher barrier for the hydrolysis of the **PA** compound could be due to the fact that tertiary amides show higher barriers than formamide and also the ring structure of **PA** could be contributing with some steric effect to a higher barriers than in *N*,*N*-dimethylacetamide. However, as the main purpose of this study is the rate acceleration due to the amide bond twist, it is important to keep analogous geometries for both twisted and planar amide as is the case for **TA** and **PA**, with the aim of isolating the effect of the amide bond.

Discussion

The general picture that comes from our calculations (see Figure 5) is that the first step of the reaction in the water-assisted stepwise mechanism, nucleophilic attack on the amide carbon, is the rate-limiting step for the acid hydrolysis of both twisted and planar amides. In the case of the twisted amide, the concerted pathway implies a higher enthalpic and free energy barrier, both in the gas phase and in solution. That is, the final aqueous free energy barriers are 10.7 kcal/mol for $TS1_s$ and 14.6 kcal/mol for TS_c, measured with respect to the unprotonated amide and hydronium molecule. In addition, the aqueous enthalpic barriers also favor $TS1_s$ (−13.5 kcal/mol) over TS_c (−10.8 kcal/mol). Besides, gas-phase free energies and enthalpies favor the stepwise mechanism over the concerted one. In summary, the acid hydrolysis of our highly twisted amide goes through a stepwise mechanism with formation of an intermediate and first step as rate limiting, contrary to the behavior previously described for the neutral hydrolysis of this same species,[44] for which a concerted pathway is preferred.

Evidence for a stepwise mechanism comes from the experiments of Kirby et al.,[21−23] who conducted hydrolysis of a twisted amide with a similar degree of twisting as TA. At slightly acidic pH, an intermediate could be trapped, which shows a very nice agreement in its geometrical properties as the one characterized with the present work (see Results). These intermediates were very rapidly cleaved upon pH neutralization, a fact that can be explained by the low barriers for intermediate cleavage $TS2_s$ in the neutral hydrolysis,[44] 9.0 kcal/mol, and the higher barrier for intermediate cleavage found at the acid hydrolysis in the present work, 17.0 kcal/mol, allowing a significant lifetime for the acid hydrolysis intermediate. It should be also emphasized that pK_a estimations for these types of twisted amides[42] points to values between 5 and 7 units, indicating that the acid hydrolysis regime for highly twisted amides is accessible at only slightly acidic pH values.

On the other hand, Wang et al.[20] have determined the enthalpic and free energy barriers for the hydrolysis of a highly twisted amide. The values are 10.3 kcal/mol for $\Delta H^{\ddagger}$, and there is a quite high entropy induced barrier of 5−6 kcal/mol, as expected for highly ordered transition states with various protons in flight. These experimental barriers are reflecting the water attack requirements on the already protonated amide[20] and are therefore to be compared to our values with $TAH^+ + 2(H_2O)$ as reference. Taking into account $TS1_s$, we obtain an enthalpic barrier of 5.1 kcal/mol in the gas phase and 16.7 kcal/mol in solution, whereas the free energy barriers are 27.8 and 39.6 kcal/mol in gas phase and aqueous phase, respectively. Thus, our calculated barriers in the aqueous phase are significantly larger than the experimental ones, specially after entropic contributions are considered. This behavior has also been observed in the comparison of previous theoretical calculations and experimental values.[64] There could be several reasons for the observed differences. First, the exact values of the aqueous barriers are highly sensitive to bulk solvent effects, and small variations in the specific solvation free energies for each of the charged species can lead to substantial differences in the actual values of the barriers. Besides, the high entropic penalties for the reaction observed in the calculations are partially due to the highly ordered nature of our transition states, but also they are due to the big loss of translational and rotational degrees of freedom when going from the three infinitely separated isolated reactants (protonated amide plus two water molecules) to the supramolecular transition state structure. Our calculations describe the separated reactants as isolated entities with non-constrained translational and rotational motions, i.e., leading to a very high entropy. However, the solute reactants and water molecules in a real system will not have such a degree of freedom due to interactions with nearby solvent molecules. In this sense, a more realistic reference state for the calculations could then be some type of hydrogen-bonded supracomplex, which could be characterized with simulations with a significant amount of specific solvent molecules around the amide solute.[40,66] Moreover, several such complexes may coexist and a proper free energy evaluation might require a statistical analysis that takes into account configuration averages. In this sense, ab initio calculations combined with dielectric continuum models and QM/MM molecular dynamics simulations in which the reference state or reactant is taken to be a hydrogen-bonded complex between formamide and several water molecules has been recently reported[55] for the neutral hydrolysis of formamide, obtaining an excellent agreement between the theoretical and experimental pseudo-first-order kinetic constant for the rate-limiting step.

Nevertheless, our main interest is to describe the rate acceleration of the hydrolysis of the twisted amide versus the planar amide, i.e., determine relative barriers ($\Delta\Delta G$) between closely related reactions with analogous definitions of reactants for both hydrolysis. One then can expect a suitable cancellation of methodological errors. In this sense, the choice of the unprotonated amide plus fully separated hydronium and water molecules has the advantage of being a clear reference state for both amide reactants. Kinetic studies have revealed that the acid hydrolysis of highly twisted amides measured for a series of highly twisted anilides is 11 orders of magnitude faster than the reactions with planar *N*-methylacetanilide,[2] which corresponds to differences in k_1/K_a values (that is, both the protonation (K_a) and hydrolytic (k_1) steps are involved). After the inherent differences in basicity of anilides and the amides treated in this work are considered,[67] this value implies a differential in free

TABLE 6: Relative Δ*H* and Δ*G* Values of the Different Transition States between the Planar and Twisted Amides in kcal/mol for the Structures Optimized in Gas Phase and in Solution (in bold), for Both the Nonassisted and Water-Assisted Reactions

	ΔH_{twist}	ΔH_{planar}	$\Delta\Delta H$	ΔG_{twist}	ΔG_{planar}	$\Delta\Delta G$
			Nonassisted			
$TS1_s$	−28.4	−14.7	13.7	−15.3	−1.6	13.7
	9.3	**25.3**	**16.0**	**22.8**	**38.3**	**15.5**
$TS2_s$	−49.9	−25.6	24.3	−37.4	−13.6	23.8
	−10.7	**11.7**	**22.4**	**1.5**	**23.1**	**21.6**
			Water Assisted			
$TS1_s$	−58.3	−34.0	24.3	−34.3	−10.2	24.1
	−13.5	**11.2**	**24.7**	**10.7**	**35.2**	**24.5**
$TS2_s$	−71.0	−50.5	20.5	−47.1	−27.5	19.6
	−21.3	**−0.3**	**21.0**	**1.5**	**22.8**	**21.3**

energy barrier ($\Delta\Delta G^{\ddagger}$) of 21.4 kcal/mol with unprotonated amide as reference. In Table 6, the theoretical data for the Δ*H* and Δ*G* in the assisted and nonassisted mechanism are collected. Our calculated value for the Δ*G* in aqueous phase when the rate-limiting transition state $TS1_s$ is considered is 24.5 kcal/mol, in reasonable agreement with the experimental estimates.Thus it seems that our model systems for the hydrolysis of a highly twisted amide are capturing the essential features of the distinct reactivity of twisted amides versus planar amides, although to reach quantitative agreement for the absolute barriers for each reaction probably better models are required, including a higher number of explicit water molecules and more accurate solvation models. It is remarkable that the values of Δ*H* and Δ*G* are similar for each reaction type, indicating that differential entropic effects between planar and twisted amide reactions are small. In addition, gas-phase and aqueous-phase Δ*H* and Δ*G* values for each reaction type are also very similar. For example, the gas-phase Δ*G* for the water-assisted $TS1_s$ is 24.1 kcal/mol versus 24.5 kcal/mol in solution. Notice that this small bulk solvent effect in the evaluation of Δ*G* makes our numbers less sensible to errors in evaluating the bulk solvation free energies. Finally, there is a high sensitivity of Δ*H* and Δ*G* values on the presence of the assistant water molecule. Thus, the value of the rate acceleration for nonassisted mechanism ($\Delta\Delta G_{aq} = 15.5$ kcal/mol) is substantially lower than that for the water-assisted mechanism ($\Delta\Delta G_{aq} = 24.5$ kcal/mol). This indicates that hydrolysis of the twisted amide is more stabilized by an extra explicit water molecule than the hydrolysis of the planar amide.

Comparison with Neutral and Alkaline Hydrolysis of Twisted Amide

In a series of papers,[42−44] we have completed the study of the rate acceleration due to the twisting of the amide bond in various pH regimes: alkaline,[43] neutral,[44] and acidic hydrolysis in the present paper. In each case, we have compared the hydrolysis of a highly twisted amide TA with its planar analogue PA. On the basis of these calculations, we have observed a rich and complex chemistry for the hydrolysis of our model highly twisted amide as a function of pH. At alkaline medium, an stepwise mechanism is observed for the hydrolysis of TA with both steps of the reaction showing similar barriers after the inclusion of the assistant water molecule.[43] Taking the first step of the reaction as the rate-limiting one, a moderate rate acceleration ($\Delta\Delta G \approx 7$ kcal/mol) with respect to analogous planar amides was observed. At neutral pH, however, a concerted pathway is the lowest-energy mechanism which leads to higher rate acceleration with respect to planar amides than in alkaline pH ($\Delta\Delta G \approx 12$ kcal/mol). Finally, at acidic medium, a stepwise mechanism is again the favored mechanism, in this case it is clearly the first step of the reaction the rate-limiting step. In addition, the acid hydrolysis shows the highest rate acceleration ($\Delta\Delta G \approx 24$ kcal/mol, measured with the unprotonated amide as reference reactant), due to both a lack of $n_N \rightarrow \pi^*_{CO}$ resonance and to a higher basicity of the twisted amides. These results are consistent with the structures that Kirby et al. had synthesized for the similar twisted amide 1-aza-2-adamantanone[22] (depicted in Figure 1). They found that when the TA was dissolved in water, it rapidly hydrolyzed to give the cleavage of the C−N bond, but at acidic conditions they were able to characterize a structure equivalent to Int_s. That is consistent with our theoretical results: at neutral pH the hydrolysis takes place in one concerted step (without forming an intermediate), but at acidic pH a stepwise mechanism is involved with intermediate formation.

TABLE 7: Δ*ΔG* along the Entire pH Range for the Water-Assisted Hydrolysis Reaction[a]

	acidic stepwise TS1	neutral[b] concerted TS_c	alkaline[c,d] stepwise TS1
$\Delta\Delta H_{gas}$	24.3	8.0	
$\Delta\Delta G_{gas}$	24.1	7.1	4.9
$\Delta\Delta H_{aq}$	24.7	12.8	
$\Delta\Delta G_{aq}$	24.5	12.5	7.0

[a] The mechanisms and rate-limiting steps are referred to TA. [b] Taken from ref 44. [c] Taken from ref 43. [d] We did not calculate the enthalpic contribution in solution.

The degree of rate acceleration due to the torsional catalysis is also highly influenced by the media (see Table 7). The highest acceleration is observed for the acid medium, and the lowest for the alkaline one. This is so, since in the acidic medium the inherent higher reactivity of the amide in twisted species is combined with the higher basicity of the amide nitrogen upon twisting and therefore a more favored protonation. In fact, our estimations for the pK_a of highly twisted amides[42] point to values between 5 and 7 pK_a units. Thus, the acid hydrolysis of twisted amides is accessible to even relatively high pH values, almost in the neutral or slightly acidic pH range.

In summary, although the kinetics of an undistorted amide shows a picture where the highest rates are obtained at alkaline or acidic media and much lower rates at neutral media,[68] the rate acceleration due to the twist of the amide bond increases as the pH decreases, because of a combination of increased reactivity amide carbon and higher basicity of the amide nitrogen. In fact, the change in the basicity properties in amides upon twisting is key to understand the differential mechanistic picture along the different pH ranges. The torsion of the amide bond and loss of $n_N \rightarrow \pi^*_{CO}$ resonance leads to profound changes in the protonation properties of amides, favoring N-protonation and showing pK_a values between 5 and 7 for the highly twisted amides. This makes a concerted pathway to be favored in the neutral hydrolysis[44] since it implies a protonation at the nitrogen in the corresponding transition state. Regarding acid hydrolysis, the change in basicity of nitrogen coupled with the loss of $n_N \rightarrow \pi^*_{CO}$ resonance leads to the highest rate accelerations of the twisted amides with respect to undistorted amides (taking the unprotonated amide as reference) and leads to a different pathway with an initial N-protonation of the twisted amide, instead of the O-protonation as in undistorted amides. All these data together give a coherent account and lies the theoretical basis for the important rate accelerations observed upon torsion of the amide bond. We also emphasize that in certain cases (acid hydrolysis stepwise mechanism, and

neutral hydrolysis concerted mechanism) the resultant mechanism is more sensible than the hydrolysis of undistorted amides toward the presence of an auxiliary water acting as a bridge in the proton transfer process, indicating that torsion of the amide bond is not sufficient by itself in leading to an efficient cleavage of the amide bond, but its effect should be accompanied by acid/base catalyst which helps reducing barriers for the in flight protons at the transition states. This clearly sets up a limit to the potential of torsional catalysis *per se* like in catalytic antibodies if it is not accompanied by a proper acid/base catalytic mechanism in turn. One should bear in mind that the torsionally induced higher reactivity of the amide can lead to a higher dependence of the hydrolytic mechanism in a properly located acid catalyst for N-protonation.

Concluding Remarks

In summary, our calculations reveal that the acid hydrolysis of highly twisted amides are subject to a stepwise mechanism with formation of an intermediate. The main difference between this mechanism and the one displayed by undistorted amides is that the initial N-protonation of the former leads to a very activated amide bond. Therefore, high values for the corresponding $\Delta\Delta H^{\ddagger}$ and $\Delta\Delta G^{\ddagger}$ were determined. There is also an intricate dependence of the preferred mechanism as a function of pH: *stepwise mechanism is predicted for acid and alkaline hydrolysis and concerted for neutral hydrolysis*. We remark that the acid hydrolysis regime for highly twisted amide can be reached at very high pH values, since the pK_a values of these twisted compounds lie close to 6−7.[42] The results shown in this paper and in previous works[42−44] lead to the description of an intriguing chemistry and complex mechanistic picture for the hydrolytic mechanism of highly twisted amides as compared to undistorted analogues, allowing for a better understanding of the substantial rate accelerations found experimentally for this set of compounds, not only as a results of lower rate limiting barriers but also as a consequence of important effect of the twist of the amide bond in the nature of the mechanisms involved in the hydrolysis.

Acknowledgment. This research was funded by Euskal Herriko Unibertsitatea (the University of the Basque Country), Gipuzkoako Foru Aldundia (the Provincial Government of Guipuzkoa), Eusko Jaurlaritza (the Basque Government), and the Spanish Office for Scientific Research. J.I.M. thanks the University of the Basque Country for a predoctoral grant. The SGI/IZO-SGIker UPV/EHU (supported by the National Program for the Promotion of Human Resources within the National Plan of Scientific Research, Development and Innovation−Fondo Social Europeo and MCyT) is gratefully acknowledged for generous allocation of computational resources.

References and Notes

(1) Brown, R.; Bennet, A.; Slebocka-Tilk, H. *Acc. Chem. Res.* **1992**, *25*, 482−488.
(2) Brown, R. S. In *The Amide Linkage*: *Selected Structural Aspects in Chemistry, Biochemistry and Materials Science*; Greenberg, A., Breneman, C. M., Liebman, J. F., Eds.; John Wiley Sons: New York, 2000.
(3) Kahne, D.; Still, W. C. *J. Am. Chem. Soc.* **1988**, *110*, 7529−7534.
(4) Bennet, A.; Somayaji, V.; Brown, R.; Santarsiero, B. D. *J. Am. Chem. Soc.* **1991**, *113*, 7563−7571.
(5) Somayaji, V.; Brown, R. S. *J. Org. Chem.* **1986**, *51*, 2676−2686.
(6) Greenberg, A.; Moore, D. T.; DuBois, T. D. *J. Am. Chem. Soc.* **1996**, *118*, 8658−8668.
(7) Romanelli, A.; Shekhtman, A.; Cowburn, D.; Muir, T. W. *Proc. Natl. Acad. Sci. U.S.A.* **2004**, *101*, 6397−6402.
(8) Poland, B. W.; Xu, M. Q.; Quiocho, F. A. *J. Biol. Chem.* **2000**, *275*, 16408−16413.
(9) Schumann, M.; Lopez, X.; Karplus, M.; Gouverneur, V. *Tetrahedron* **2001**, *57*, 10299−10307.
(10) Mannfors, B. E.; Mirkin, N. G.; Palmo, K.; Krimm, S. *J. Phys. Chem. A* **2003**, *107*, 1825−1832.
(11) Gilli, G.; Bertolasi, V.; Belluccu, F.; Ferretti, V. *J. Am. Chem. Soc.* **1986**, *108*, 2420−2424.
(12) Wiberg, K.; Laidig, K. *J. Am. Chem. Soc.* **1987**, *109*, 5935.
(13) Wiberg, K.; Laidig, K. *J. Am. Chem. Soc.* **1992**, *114*, 831.
(14) Wiberg, K.; Hadad, C.; Rablen, P.; Cioslowski, J. *J. Am. Chem. Soc.* **1992**, *114*, 8644.
(15) Wiberg, K. B.; Rablen, P. R. *J. Am. Chem. Soc.* **1993**, *115*, 9234−9242.
(16) Wiberg, K. B.; Rablen, P. R. *J. Am. Chem. Soc.* **1995**, *117*, 2201−2209.
(17) Wiberg, K. B.; Rush, D. J. *J. Am. Chem. Soc.* **2001**, *123*, 2038−2046.
(18) Blackburn, G. M.; Plackett, J. D. *J. Chem. Soc., Perkin Trans. 2* **1972**, 1366−1371.
(19) Blackburn, G. M.; Skaife, C. J.; Kay, I. T. *J. Chem. Res.* **1980**, 294−295.
(20) Wang, Q. P.; Bennet, A. J.; Brown, R. S.; Santarsiero, B. D. *J. Am. Chem. Soc.* **1991**, *113*, 5757−5765.
(21) Kirby, A. J.; Komarov, I. V.; Wothers, P.; Feeder, N. *Angew. Chem., Int. Ed. Engl.* **1998**, *37*, 785−786.
(22) Kirby, A. J.; Komarov, I. V.; Feeder, N. *J. Am. Chem. Soc.* **1998**, *120*, 7101−7102.
(23) Kirby, A. J.; Komarov, I. V.; Feeder, N. *J. Chem. Soc., Perkin Trans. 2* **2001**, 522−529.
(24) Guthrie, J. *J. Am. Chem. Soc.* **1974**, *96*, 3608.
(25) Oie, T.; Loew, G. H.; Burt, S. K.; Binkley, J. S.; D.MacElroy, R. *J. Am. Chem. Soc.* **1982**, *104*, 6169−6174.
(26) Weiner, S. J.; Singh, U. C.; Kollman, P. *J. Am. Chem. Soc.* **1985**, *107*, 2219−2229.
(27) Krug, J.; Popelier, P.; Bader, R. F. W. *J. Phys. Chem.* **1992**, *96*, 7604−7616.
(28) Jensen, J. H.; Baldridge, K. K.; Gordon, M. S. *J. Phys. Chem.* **1992**, *96*, 8340−8351.
(29) Antonczak, S.; Ruiz-López, M. F.; Rivail, J. L. *J. Am. Chem. Soc.* **1994**, *116*, 3912−3921.
(30) Antonczak, S.; Ruiz-López, M. F.; Rivail, J. L. *J. Mol. Model.* **1997**, *3*, 434.
(31) Dobbs, D. K.; Dixon, D. A. *J. Phys. Chem.* **1996**, *100*, 3965−3973.
(32) Rauk, A.; Glover, S. A. *J. Org. Chem.* **1996**, *61*, 2337−2345.
(33) Hori, K.; Kamimura, A.; Ando, K.; Mizumura, M.; Ihara, Y. *Tetrahedron* **1997**, *53*, 4317−4330.
(34) Kallies, B.; Mitzner, R. *J. Mol. Model.* **1998**, *4*, 183−196.
(35) Zheng, Y. J.; Ornstein, R. L. *J. Mol. Struct.* **1998**, *429*, 41−48.
(36) Stanton, R. V.; Perakyla, M.; Bakowies, D.; Kollman, P. A. *J. Am. Chem. Soc.* **1998**, *120*, 3448−3457.
(37) Bakowies, D.; Kollman, P. A. *J. Am. Chem. Soc.* **1999**, *121*, 5712−5726.
(38) Glover, S. A.; Rauk, A. *J. Org. Chem.* **1999**, *64*, 2340−245.
(39) Strajbl, M.; Florián, J.; Warshel, A. *J. Am. Chem. Soc.* **2000**, *122*, 5354−5366.
(40) Chalmet, S.; Harb, W.; Ruiz-López, M. F. *J. Phys. Chem. A* **2001**, *105*, 11574−11581.
(41) Greenberg, A.; Venanzi, C. A. *J. Am. Chem. Soc.* **1993**, *115*, 6951−6957.
(42) Mujika, J. I.; Mercero, J. M.; Lopez, X. *J. Phys. Chem. A* **2003**, *107*, 6099−6107.
(43) Lopez, X.; Mujika, J.; Blackburn, G.; Karplus, M. *J. Phys. Chem. A* **2003**, *107*, 2304−2315.
(44) Mujika, J. I.; Mercero, J. M.; Lopez, X. *J. Am. Chem. Soc.* **2005**, *127*, 4445−4453.
(45) Frisch, M. J.; Trucks, G. W.; Schlegel, H. B.; Scuseria, G. E.; Robb, M. A.; Cheeseman, J. R.; Zakrzewski, V. G.; Montgomery, J. A.; Stratmann, R. E.; Burant, J. C.; Dapprich, S.; Millam, J. M.; Daniels, A. D.; Kudin, K. N.; Strain, M. C.; O. Farkas, J. T.; Barone, V.; Cossi, M.; Cammi, R.; Mennucci, B.; Pomelli, C.; Adamo, C.; Clifford, S.; Ochterski, J.; Petersson, G. A.; Ayala, P. Y.; Cui, Q.; Morokuma, K.; Malick, D. K.; Rabuck, A. D.; Raghavachari, K.; Foresman, J. B.; Cioslowski, J.; Ortiz, J. V.; Stefanov, B. B.; Liu, G.; Liashenko, A.; Piskorz, P.; Komaromi, I.; Gomperts, R.; Martin, R. L.; Fox, D. J.; Keith, T.; Al-Laham, M. A.; Peng, C. Y.; Nanayakkara, A.; Gonzalez, C.; Challacombe, M.; Gill, P. M. W.; Johnson, B. G.; Chen, W.; Wong, M. W.; Andres, J. L.; Head-Gordon, M.; Replogle, E. S.; Pople, J. A. *Gaussian 98*, revision a.2; Gaussian, Inc.: Pittsburgh, PA, 1998.
(46) Vosko, S. H.; Wilk, L.; Nusair, M. *Can. J. Phys.* **1980**, *58*, 1200.
(47) Becke, A. D. *Phys. Rev. A* **1988**, *38*, 3098.
(48) Lee, C.; Yang, W.; Parr, R. G. *Phys. Rev. B* **1988**, *37*, 785.
(49) Becke, A. D. *J. Chem. Phys.* **1993**, *98*, 5648.

(50) Mercero, J.; Matxain, J.; Lopez, X.; York, D.; Largo, A.; Eriksson, L.; Ugalde, J. *Int. J. Mass Spectrom.* **2005**, *240*, 37−99.

(51) Hehre, W.; Radom, L.; Schleyer, P.; Pople, J. *Ab Initio Molecular Orbital Theory*; Wiley-Interscience: New York, 1986.

(52) Tidor, B.; Karplus, M. *J. Mol. Biol.* **1994**, *238* (3), 405−414.

(53) Iché-Tarrat, N.; Barthelat, J.-C.; Rinaldi, D.; Vigroux, A. *J. Phys. Chem. B* **2005**, *109*, 22570−22580.

(54) Ayala, P. Y.; Schlegel, H. B. *J. Chem. Phys.* **1998**, *108*, 2314−2325.

(55) Gorb, L.; Asensio, A.; Tuñon, I.; Ruiz-López, M. F. *Chem. Eur. J.* **2005**, *11*, 6743−6753.

(56) Foresman, J. B.; Keith, T. A.; Wiberg, K. B.; Snoonian, J.; Frisch, M. J. *J. Phys. Chem.* **1996**, *100*, 16098.

(57) Barone, V.; Cossi, M.; Tomasi, J. *J. Chem. Phys.* **1997**, *107*, 3210−3221.

(58) Ferretti, V.; Bertolasi, V.; Gilli, P.; Gilli, G. *J. Phys. Chem.* **1993**, *97*, 13568−13574.

(59) The introduction of an explicit water molecule hydrogen bonded to the $N-H^+$ proton can have a sizable effect in the C_1-N bond length. In the gas phase, the bond length is shortened from 1.553 to 1.532 Å, and in bulk solvent (modeled by SCI−PCM) from 1.529 to 1.516 Å. However, calculations not shown in this paper demonstrated that this specific microsolvation of the $N-H^+$ proton by a water molecule has a small effect on the reaction barrier for the rate-limiting step $TS1_s^W$, and therefore, its effect is not considered in the paper.

(60) Guthrie, J. P. *J. Am. Chem. Chem.* **1974**, *96*, 3608−3615.

(61) Langlois, S.; Broche, A. *Bull. Soc. Chim. Fr.* **1964**.

(62) Bolton, P. D. *Aust. J. Chem.* **1966**, *19*, 1013.

(63) Bolton, P. D.; Jackson, G. L. *Aust. J. Chem.* **1971**, *24*, 969.

(64) Slebocka-Tilk, H.; Sauriol, F.; Monette, M.; Brown, R. *Can. J. Chem.* **2002**, *80*, 1343−1350.

(65) Manojkumar, T. K.; Suh, S. B.; Oh, K. S.; Cho, S. J.; Cui, C.; Zhang, X.; Kim, K. S. *J. Org. Chem.* **2005**, *70*, 2651−2659.

(66) Zahn, D. *Chem. Phys.* **2004**, *300*, 79−83.

(67) The 11 orders of magnitude in rate acceleration corresponds to differences in the ratio of k_1/K_a values between distorted anilides and *N*-methylacetanilide,[2] and therefore, they correspond to a difference in both the protonation (K_a) and hydrolytic (k_1) steps. As a consequence, a proper estimation of the $\Delta\Delta G^{\ddagger}$ should also take into account the differences in acidities between anilides and the amides modeled in the present work. On the basis of our own estimations of the pK_a values for these compounds,[42] the highly twsited amide TA modeled in this work shows a pK_a of 6.5, whereas the corresponding distorted anilide has a pK_a of 2.9. In addition, the pK_a of *N*,*N*-dimethylacetamide, representative of the pK_a of a tertiary planar amide, is −0.28, whereas the pK_a of *N*-methylacetanilide is 0.61.[2] When these differences in the acidity constants are considered, an estimate of 15.5 orders of magnitude in rate acceleration corresponding to k_1/K_a ratios is obtained, which implies a $\Delta\Delta G^{\ddagger}$ of 21.4 kcal/mol (if $T = 300$ K is considered) and the unprotonated amide is taken as a reference for the evaluation of free energy barriers, in reasonable agreement with our calculated 24.5 kcal/mol.

(68) Smith, R. M.; Hansen, D. E. *J. Am. Chem. Soc.* **1998**, *120*, 8910−8913.